Anais da Academia Brasileira de Ciências (2019) 91(1): e20170397
(Annals of the Brazilian Academy of Sciences)
Printed version ISSN 0001-3765 / Online version ISSN 1678-2690
http://dx.doi.org/10.1590/0001-3765201920170397
www.scielo.br/aabc | www.fb.com/aabcjournal

# The performance of the (U+Th)/He thermochronology laboratory at UNESP Rio Claro, Brazil

**MARLI C. SIQUEIRA-RIBEIRO[1], DANIELI F.C. MARIN[1], PETER C. HACKSPACHER[1] and FINLAY M. STUART[2]**

[1]Departamento de Petrologia e Metalogenia, Universidade Estadual Paulista, Caixa Postal 178, 13506-900 Rio Claro SP, Brazil
[2]Scottish Universities Environmental Research Centre-Isotope Geosciences Unit, SUERC, East Kilbride, G75 0QF, Scotland, UK

*Manuscript received on October 16, 2017; accepted for publication on July 13, 2018*

**How to cite**: SIQUEIRA-RIBEIRO MC, MARIN DFC, HACKSPACHER PC AND STUART FM. 2019. The performance of the (U+Th)/He thermochronology laboratory at UNESP Rio Claro, Brazil. An Acad Bras Cienc 91: e20170397. DOI 10.1590/0001-3765201920170397.

**Abstract:** We have developed the first laboratory for (U-Th-Sm)/He thermochronology measurements in South America. Helium is measured using a high-sensitivity magnetic sector mass spectrometer (GVI-Helix-SFT) and a double focusing single collector inductively coupled plasma mass spectrometer (Thermo Scientific ELEMENT2) is used for U, Th and Sm determinations. Repeated analyses of fragments of Durango fluorapatite crystals yields an average age of 31.6 ± 1.6 Ma (2σ) (n=62). This overlaps the long-term average of Durango fluorapatite measured in laboratories worldwide. The analysis of multiple single apatite crystals of a Precambrian basement sample from Serra do Mar, southeastern Brazil, yields an average He age (60.5 ± 8.7 Ma; n=8) that overlaps that measured in the SUERC laboratory (59.6 ± 3 Ma; n=3). This confirms that the UNESP laboratory is capable of routinely measuring the (U-Th-Sm)/He ages of single apatite crystals.

**Key words:** (U-Th)/He dating, He calibration, Noble Gas, Serra do Mar AHe ages.

## INTRODUCTION

(U-Th-Sm)/He dating of minerals relies on the production of $^{4}$He from $^{235}$U, $^{238}$U, $^{232}$Th, and $^{147}$Sm via alpha decay. The radiogenic $^{4}$He diffuses at relatively low temperatures (<300°C) in many U- and/or Th-bearing accessory minerals (e.g., Farley 2002, Reiners 2002), except some minerals has high closure temperature (e.g., baddeleyite). (U-Th-Sm)/He ages are now routinely determined on a range of minerals that contain measureable U and Th, principally apatite and zircon. (U-Th-Sm)/He ages are typically interpreted as cooling ages, with each mineral assigned a closure temperature based on the cooling rate, grain size (or its effective diffusion dimension), and the temperature-dependent diffusivity of $^{4}$He in the mineral (Dodson 1973). The non-uniform distribution of the parent elements can affect diffusive He loss by modifying the spatial distribution of He concentration in crystal (e.g., Farley 2002, Meesters and Dunai 2002, Dobson et al. 2008) and by eliminating age dispersion induced by using an alpha ejection correction to ages assuming homogeneous parent element distribution. Variation in the extent of radiation damage and grain size can cause dispersion of ages of single minerals from the same rock. The accumulation of radiation damage

Correspondence to: Marli Carina Siqueira-Ribeiro
E-mail: carinasr@unesp.br
ORCid: https://orcid.org/0000-0001-9727-0370

in apatite crystals has been shown to impede He diffusion, such that single apatite crystals with higher parent element concentrations have higher closure temperatures and record older ages (e.g., Shuster et al. 2006, Gautheron et al. 2009). Larger apatite crystals have a greater effective diffusion dimension and therefore retain a higher proportion of the radiogenic He than smaller apatite (Farley 2002). The effect of radiation damage and grain size is most pronounced in rocks that have spent significant lengths of time at temperatures close to the closure temperature. This may be apparent as a positive correlation between He age and eU (Flowers et al. 2009, Gautheron et al. 2009) or crystal size (Reiners and Farley 2001).

Apatite He thermochronology has been used to study the exhumation-induced cooling history of samples in tectonically active and passive margins regions (House et al. 1998, Farley et al. 2002, Persano et al. 2002, Ehlers and Farley 2003), and is particularly powerful when combined with apatite fission track and zircon (U+Th)/He thermochronology (e.g. Kirstein et al. 2006, Merten et al. 2010, Macaulay et al. 2014).

In this study we report the hardware and the procedure for determining (U+Th)/He ages in single apatite crystals at the new facility at UNESP, Rio Claro, Brazil. We report age determinations of the Durango fluorapatite reference mineral to demonstrate the ability of the laboratory to generate accurate apatite (U-Th-Sm)/He ages (AHe). Furthermore, we report the He ages of apatite from the Serra do Mar southeastern Brazil and compare with analyses done in the long-established laboratory at Scottish Universities Environmental Research Centre (SUERC) in UK.

## INSTRUMENTATION

### HELIUM ANALYTICAL SYSTEM

Single apatite crystals are packed into Pt tubes and loaded into 3 mm deep recesses in a Cu sample pan. Helium is extracted from apatite using a 960 nm diode laser heating system (Fusions 960, Photon Machines) (Figure 1a). A sapphire viewport is used to minimise the inward diffusion of atmosphere-derived He. The laser beam intensity, spot size and beam movement are computer controlled.

The noble gas extraction and purification system (Figure 1b) is made of internally polished stainless steel tubing. It is equipped with two SAES TiZr getters (NP10) and a liquid nitrogen-cooled charcoal trap. Ultra-high vacuum ($\sim 10^{-9}$ mbar) is maintained by a combination of a turbo-molecular pump and a triode ion pump.

Helium abundances are measured using a Helix-SFT magnetic sector mass spectrometer (GV Instruments) (Figure 1c). It is equipped with a modified Nier-type electron bombardment source with x and z focusing. All source parameters, including the 4.5 kV acceleration potential, are computer controlled, and ion beams are focused manually. A sensitivity of $1.84 \times 10^{8}$ V/cm$^3$ STP at 450 μA trap current for $^4$He has been measured using a known amount of He in calibration reservoir used in the SUERC laboratory (Foeken et al. 2006). The $^4He^+$ beam intensity is measured using a Faraday detector fitted with a $10^{11}\Omega$ resistor. An embedded personal computer runs a real time operating system that controls all the electronics via a fiber optic loop. This unit sends all data before they are passed back to the Windows XP PC running the primary interface software.

### U AND Th ANALYSIS SYSTEM

The uranium and thorium content of all samples are measured using a double focusing single collector inductively coupled plasma mass spectrometer (ICP-MS) (Thermo Scientific ELEMENT2). The sample introduction system is set with a micromist concentric combined with a Twinnabar™ spray chamber, both made of borosilicate glass. The ion source is configured with torch and 1.75 mm

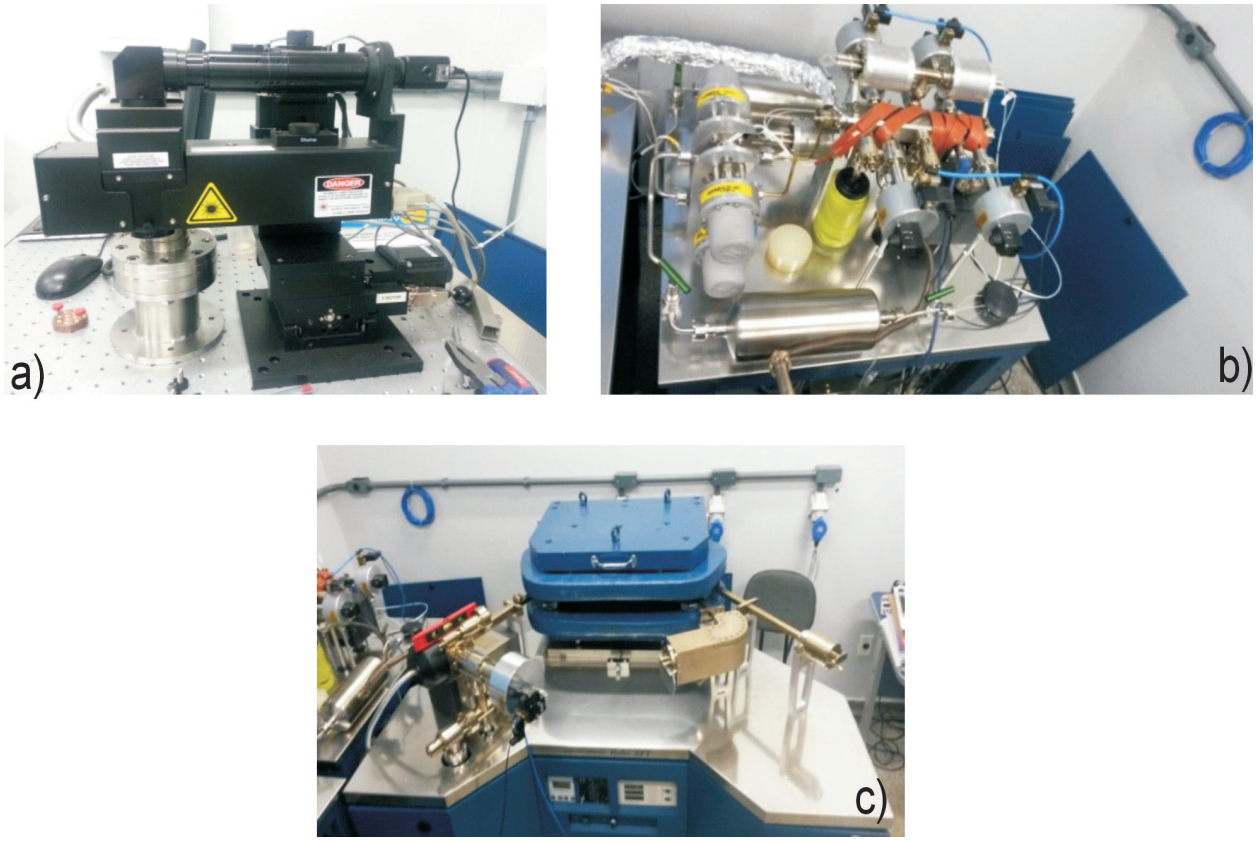


**Figure 1 -** Photograph of the gas extraction, purification and measurement system; (**a**) laser heating system, (**b**) gas purification bench, and (**c**) Helix-SFT noble gas mass spectrometer.

quartz injector and the interface region have two nickel cones (sampler/skimmer) with diameters of 1.2 and 0.4 mm, respectively. Low resolution and electrostatic peak jumping mode ensure high sensitivity and adequate measurement precision to isotope ratios. $^{238}U$ sensitivity is checked using a tuning solution with a concentration of 1 µg/L which usually yields 1.4 to 2.0 x $10^6$ cps (counts per second).

## ANALYTICAL PROCEDURES

Single crystals of apatite are hand-picked to be free from visible fluid and mineral inclusions, cracks and fractures using a Zeiss Discovery V8® stereoscopic microscope at $80^x$ magnification. The crystal length, termination lengths and hexagonal crystals widths were determined using an AxionVision® software. Individual crystals are packed into 1 x 1 mm Pt tubes that are crimped closed at each end. The Pt tubes are loaded into a 60 hole Cu sample pan.

System sensitivity is determined by analysing $^4He$ delivered from a 0.1 ml pipette from a 2,200 cc reservoir bottle that contains 5.7 x $10^{-4}$ cc He. The reservoir bottle was filled at UNESP with essentially pure $^4He$ by degassing a zircon from Sri Lankan similar to those reported by Nasdala et al. (2013). This reservoir was calibrated against a standard reservoir from SUERC (Foeken et al. 2006).

Sample and calibration gas is purified using two SAES TiZr getters and liquid nitrogen-cooled charcoal trap prior to analysis. Helium is measured in a 30-cycle run using the Ion Vantage software. Baselines are measured over 30 seconds with an

integration time of 5 seconds immediately after gas inlet during equilibration prior to analysis. Each data collection cycle has a period of 12 seconds and the total data collection time is 320 seconds. The near-linear evolution of He in the mass spectrometer implies that the extracted gases are sufficiently purified during gas clean-up procedure.

The precision of He measurements is determined by repeated analysis of the $^{4}$He standard. Figure 2 shows a calibration standard data collection output. The beam intensity of the $^{4}$He decreases with the time showing a slight concave downward form. Repeated determinations of the He standard (n=60) yield relative standard deviation of ±0.25% (RSD).

To determine the linearity of the mass spectrometer, known amounts of $^{4}$He have been analysed over the range 0.59 to 6.6 x $10^{-8}$ cc that encompasses the complete range of He from single apatite (and zircon) crystals. There is no significant change in sensitivity over the measured range of He (Figure 3).

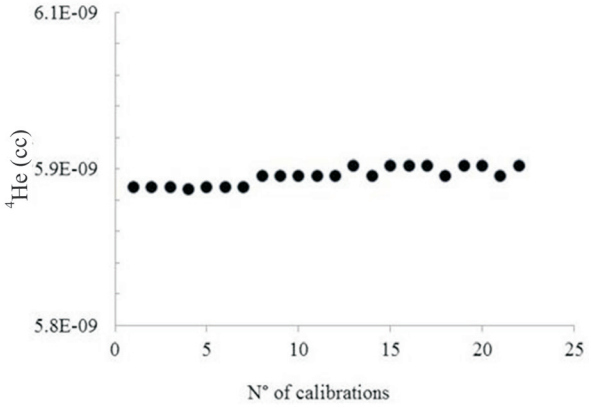


**Figure 2 -** The results of repeated measurements of the $^{4}$He calibration standard.

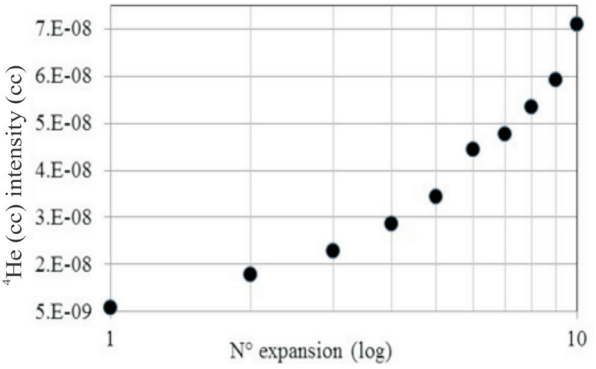


**Figure 3 -** Plots showing the expansion experiment using 10 shots of He from the standard reservoir.

## APATITE He, U, AND Th ANALYSIS PROCEDURES

Single apatite crystals are loaded into Pt tubes and placed into holes in the Cu sample pan. Prior to sample analysis, the laser chamber and connecting flexi-tube are degassed at approximately 100°C for 4 hours, which reduces H, $CH_4$ and $H_2O$ background levels. Laser heating of empty Pt tubes (hot blanks) yields He beam intensities that are close to system background levels (<6 x $10^{-12}$ ccSTP n=30).

Apatites are outgassed in vacuum by rastering the focused diode laser beam onto Pt foil packets for 1 minute at 650-730°C. This is achieved using a beam size of ~0.06 mm and the laser power of 0.03 to 0.05 W. The temperature of the Pt foils is assessed by visual observation of the colour emitted using Chromium software (Photon Machines). Small variation in the degree to Pt tubes couple with the beam is related to packet orientation. To confirm complete He extraction all samples are re-heated.

All analysis is conducted in static mode with $^{4}$He detection in Faraday cup following the same procedures of $^{4}$He determination from the standard reservoir. Each analysis takes ~16 minutes. Absolute He contents are calculated by peak height comparison to the standard He peak.

After helium extraction, the Pt tubes containing the apatite grains are placed into Teflon beakers, spiked with a $^{230}$Th, $^{235}$U and $^{149}$Sm certified solutions, and acidified with bi-distillated 5% $HNO_3$ solution. The beakers are put on a hot plate (~110°C) for 48 hours to complete grain dissolution. Thereafter, U, Th and Sm are measured by ICP-MS.

To check the purity of the reagents, several beakers with aliquots of bi-distillated 5% $HNO_3$ solution were analyzed. The "acid blank" results are typically 50-200 cps of $^{232}$Th and $^{238}$U, and 5-25 cps to $^{230}$Th and $^{235}$U. Pt foil blanks were prepared in the same way of apatite samples. The average of ~50 blank measurements is 1 pg to $^{232}$Th and 0.1 pg to $^{238}$U. Fractionation in the mass spectrometer is monitored and corrected using CRM U500 standard. 2 ng/g solution of U500 bias measured at the start and end of every analysis, and additional aliquots are interspersed every 3 samples. The reproducibility of the CRM U500 solution in 150 measurements is ~0.2% RSD.

## (U-Th-Sm)/He AGES

### DURANGO FLUORAPATITE

The Durango fluorapatite from Cerro de Mercado, Mexico is a commonly used internal reference for He thermochronology laboratories. It is largely free of fluid and mineral inclusions, and crystals in excess of a centimeter in diameter are easily obtained. Zeitler et al. (1987), Wolf et al. (1996) and Farley (2002) selected this material for their landmark studies of the diffusion of the helium in apatite. Their results demonstrate straightforward and reproducible diffusive behaviour of $^{4}$He.

The U, Th and He from the (U+Th)/He analytical system experiments of Durango fluorapatite reference material are reported in Table I and plotted in Figure 4. Seven fragments of a Durango apatite crystal supplied by SUERC (East Kilbride) and fifty-five fragments of the in-house Durango apatite (Rio Claro) were analysed.

Durango fluorapatite EK yields a mean Th/U of 26.9 ± 4.2 and mean He age of 31.9 ± 1.2 Ma (2σ). This overlaps with published analyses of this sample from the SUERC laboratory (Foeken et al. 2006). Analysis of fifty-five RC Durango apatite fragments have Th/U = 20.5 ± 3.1 and

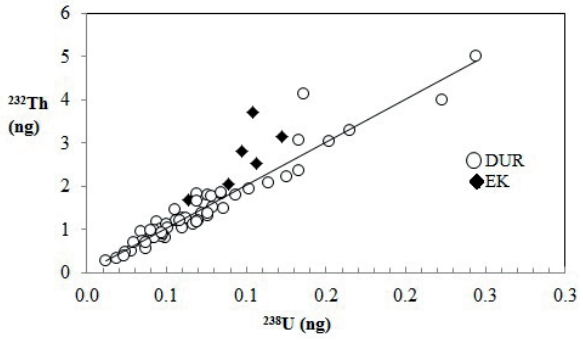


**Figure 4 -** Concentrations of $^{238}$U and $^{232}$Th in 62 fragments of the Durango fluorapatite. Black diamonds represent SUERC (EK) Durango, white circles are UNESP Rio Claro DUR UNESP (RC) Durango.

with mean apatite He age of 31.6 ± 1.7 Ma (2σ) (Table I and Figure 4). The mean He ages compare well with the equivalent value reported by, for example, CIT (32.1 ± 1.7 Ma n=11) (2σ) (House et al. 2000). It is in agreement with the accepted single-crystal sanidine-anorthoclase $^{40}$Ar/$^{39}$Ar age of 31.44 ± 0.18 Ma presented by McDowell et al. (2005). The Th/U ratios of all samples are within the range determined by *in situ* LA-ICP-MS (17.8-27.7 ppm; Boyce and Hodges 2005). The EK and RC Durango fluorapatite the Th/U ratio display a greater range, however, there is no systematic relationship between Th/U and He age. The U/Th range likely reflects grain-to-grain variability rather than possible relationship with nuclides parent volatilization (Figure 5). Importantly, our heating schedule has preserved the systematic difference in the Th/U ratio, attesting to complete retention of U and Th during laser heating between 0.3 to 0.5 W power output.

### APPLICATION OF APATITE (U-Th)/He THERMOCHRONOLOGY

In order to demonstrate the reproducibility of the procedures used to generate accurate apatite (U-Th-Sm)/He ages, several single apatite crystals from samples from the Serra do Mar southeastern Brazil, have been analysed. High quality apatite separates

**TABLE I**
**He, U and Th data for Durango fluorapatite reference material from UK (EK) and DUR UNESP (RC) (U+Th)/He thermochronology laboratory at UNESP Rio Claro.**

| Sample | $^{4}$He (cc) | $^{238}$U (ng) | $^{232}$Th (ng) | Th/U | Age (Ma) | Uncertainty |
|---|---|---|---|---|---|---|
| EK 9-14-1 | 2.82E-09 | 0.11 | 2.54 | 23.96 | 33.9 | 1.3 |
| EK 9-14-2 | 3.72E-09 | 0.10 | 3.71 | 35.65 | 30.9 | 1.2 |
| EK 9-14-3 | 2.77E-09 | 0.10 | 2.81 | 28.99 | 30.9 | 1.2 |
| EK 9-14-6 | 3.27E-09 | 0.12 | 3.14 | 25.73 | 31.9 | 1.2 |
| EK 9-14-7 | 1.74E-09 | 0.06 | 1.67 | 26.11 | 32.5 | 1.2 |
| EK 9-14-8 | 2.03E-09 | 0.09 | 2.06 | 23.09 | 30.7 | 1.2 |
| EK 9-14-9 | 1.77E-09 | 0.07 | 1.70 | 25.36 | 32.4 | 1.3 |
| DUR 9-14-2 | 1.95E-09 | 0.07 | 1.82 | 26.43 | 33.8 | 1.3 |
| DUR 9-14-3 | 1.10E-09 | 0.04 | 1.18 | 26.80 | 31.1 | 1.2 |
| DUR 9-14-4 | 1.50E-09 | 0.06 | 1.46 | 26.60 | 33.1 | 1.3 |
| DUR 9-14-5 | 4.20E-09 | 0.14 | 4.14 | 30.46 | 32.0 | 1.3 |
| DUR-10-14-2 | 9.20E-10 | 0.05 | 0.81 | 16.54 | 31.4 | 2.9 |
| DUR-10-14-3 | 9.80E-10 | 0.04 | 0.89 | 20.22 | 31.9 | 2.9 |
| DUR-10-14-09 | 9.80E-10 | 0.04 | 0.98 | 23.39 | 32.8 | 1.3 |
| DUR-10-14-12 | 8.10E-10 | 0.04 | 0.80 | 19.48 | 28.9 | 2.7 |
| DUR-10-14-13 | 2.80E-10 | 0.01 | 0.26 | 21.25 | 30.6 | 2.8 |
| DUR-10-14-14 | 9.80E-10 | 0.04 | 0.94 | 22.77 | 30.8 | 2.8 |
| DUR-10-14-16 | 1.23E-09 | 0.05 | 1.12 | 22.46 | 32.6 | 1.2 |
| DUR-10-14-17 | 1.87E-09 | 0.08 | 1.79 | 23.52 | 31.1 | 1.2 |
| DUR-10-14-21 | 5.80E-10 | 0.03 | 0.49 | 17.40 | 32.9 | 3.0 |
| DUR-10-14-22 | 8.60E-10 | 0.05 | 0.83 | 17.56 | 29.1 | 2.7 |
| DUR-10-14-23 | 2.00E-09 | 0.09 | 1.79 | 19.27 | 32.6 | 3.0 |
| DUR-10-14-24 | 1.20E-09 | 0.06 | 1.21 | 21.87 | 28.6 | 2.6 |
| DUR-10-14-27 | 1.10E-09 | 0.06 | 1.03 | 17.12 | 29.9 | 2.7 |
| DUR-10-14-29 | 2.30E-09 | 0.11 | 2.07 | 18.09 | 31.4 | 2.9 |
| DUR-10-14-30 | 1.40E-09 | 0.06 | 1.26 | 21.09 | 32.7 | 3.0 |
| DUR-10-14-31 | 1.00E-09 | 0.03 | 0.96 | 27.91 | 32.0 | 3.0 |
| DUR-10-14-32 | 1.00E-09 | 0.05 | 1.01 | 22.13 | 29.9 | 2.8 |
| DUR-10-14-33 | 8.30E-10 | 0.04 | 0.72 | 20.51 | 33.3 | 3.1 |
| DUR-10-14-34 | 1.70E-09 | 0.07 | 1.58 | 21.45 | 31.1 | 2.9 |
| DUR-10-14-35 | 3.00E-09 | 0.13 | 3.08 | 23.14 | 28.8 | 2.7 |
| DUR-10-14-41 | 1.40E-09 | 0.06 | 1.25 | 20.21 | 31.8 | 2.9 |
| DUR-10-14-43 | 9.90E-10 | 0.04 | 0.91 | 22.15 | 32.1 | 3.0 |
| DUR-10-14-44 | 1.80E-09 | 0.08 | 1.81 | 21.50 | 29.1 | 2.7 |
| DUR-10-14-46 | 7.70E-10 | 0.03 | 0.69 | 23.62 | 33.2 | 3.1 |
| DUR-10-14-48 | 1.30E-09 | 0.06 | 1.20 | 20.71 | 31.4 | 2.9 |
| DUR-11-14-1 | 8.52E-10 | 0.04 | 0.82 | 19.71 | 29.8 | 2.2 |
| DUR-11-14-2 | 4.55E-10 | 0.02 | 0.47 | 19.49 | 27.8 | 2.4 |
| DUR-11-14-7 | 6.14E-10 | 0.04 | 0.54 | 16.20 | 28.6 | 2.5 |

**TABLE I (continuation)**

| Sample | $^{4}$He (cc) | $^{238}$U (ng) | $^{232}$Th (ng) | Th/U | Age (Ma) | Uncertainty |
|---|---|---|---|---|---|---|
| DUR-11-14-8 | 1.16E-09 | 0.07 | 1.11 | 16.61 | 29.1 | 2.5 |
| DUR-11-14-9 | 3.80E-10 | 0.02 | 0.34 | 17.56 | 31.3 | 2.7 |
| DUR-11-14-10 | 9.50E-10 | 0.04 | 0.97 | 24.39 | 29.1 | 2.6 |
| DUR-1-15-1 | 3.28E-09 | 0.15 | 3.04 | 20.04 | 31.0 | 0.3 |
| DUR-1-15-2 | 1.61E-09 | 0.07 | 1.38 | 19.15 | 33.5 | 0.3 |
| DUR-1-15-3 | 1.50E-09 | 0.08 | 1.32 | 17.33 | 31.4 | 0.3 |
| DUR-1-15-4 | 2.40E-09 | 0.13 | 2.22 | 17.69 | 30.4 | 0.3 |
| DUR-1-15-5 | 2.00E-09 | 0.08 | 1.76 | 22.44 | 33.2 | 0.3 |
| DUR-1-15-6 | 1.21E-09 | 0.05 | 1.04 | 20.40 | 33.5 | 0.3 |
| DUR-1-15-7 | 2.30E-09 | 0.10 | 1.95 | 19.03 | 33.1 | 0.3 |
| DUR-1-15-8 | 1.41E-09 | 0.07 | 1.17 | 16.87 | 33.7 | 0.3 |
| DUR-1-15-9 | 1.74E-09 | 0.08 | 1.50 | 19.08 | 33.0 | 0.3 |
| DUR-1-15-10 | 9.17E-10 | 0.047 | 0.914 | 19.58 | 28.7 | 0.3 |
| DUR-2-15-1 | 1.33E-09 | 0.07 | 1.21 | 17.31 | 30.7 | 0.3 |
| DUR-2-15-2 | 5.51E-09 | 0.24 | 5.02 | 20.55 | 31.8 | 0.3 |
| DUR-2-15-3 | 2.64E-09 | 0.13 | 2.36 | 17.73 | 32.4 | 0.3 |
| DUR-2-15-5 | 1.70E-09 | 0.09 | 1.48 | 17.17 | 31.8 | 0.3 |
| DUR-2-15-6 | 2.10E-09 | 0.08 | 1.87 | 22.21 | 33.1 | 0.3 |
| DUR-3-15-2 | 4.52E-10 | 0.02 | 0.38 | 16.43 | 33.1 | 0.3 |
| DUR-3-15-4 | 3.66E-09 | 0.17 | 3.30 | 19.99 | 31.9 | 0.3 |
| DUR-3-15-7 | 9.88E-10 | 0.05 | 0.89 | 18.50 | 31.5 | 0.3 |
| DUR-3-15-9 | 1.59E-09 | 0.08 | 1.37 | 18.03 | 32.8 | 0.3 |
| DUR-4-15-1 | 8.20E-10 | 0.04 | 0.71 | 19.22 | 33.2 | 0.3 |
| DUR-4-15-2 | 1.90E-09 | 0.07 | 1.66 | 24.03 | 34.7 | 0.3 |

were taken from sample TF-685, Neoproterozoic gneiss from Angra dos Reis (RJ). Ages from the UNESP laboratory range from 44.3 to 56.0 Ma (n=8 grains), yielding an average age of 50.7 ± 6.1 Ma (2σ) (Table II). This overlaps the age (45.7 ± 2.8 Ma) (2σ) determined on 3 crystals at the SUERC thermochronology laboratory. These are consistent with previous thermochronology studies of the region (Cogné et al. 2011, 2012, Siqueira-Ribeiro et al. 2011) and will be used in future studies of the region.

AHe ages are subject to variation due to the thermal history the sample has experienced. However, the eU contend and grain size exploit to compound and enhance single-grain AHe age dispersion (Reiners and Farley 2001, Flowers et al. 2009, Gautheron et al. 2009). All grains had two terminations so crystal form is not an explanation for the age variation (Brown et al. 2013). AHe ages are listed in Table 2 and plotted in Figure 6, we plot apatite He ages from the Serra do Mar against eU and grain size in Figure 6. Our data do not show any strong positive age-grain size or age-eU relationships, where can be attributed to the combined effects of eU grain radius, and potentially other unknown factors that are contributing to single-grain AHe age dispersion.

Previous thermochronological data from SM obtained studies of the Hackspacher et al. (2004), Hiruma et al. (2010), Cogné et al. (2011, 2012),

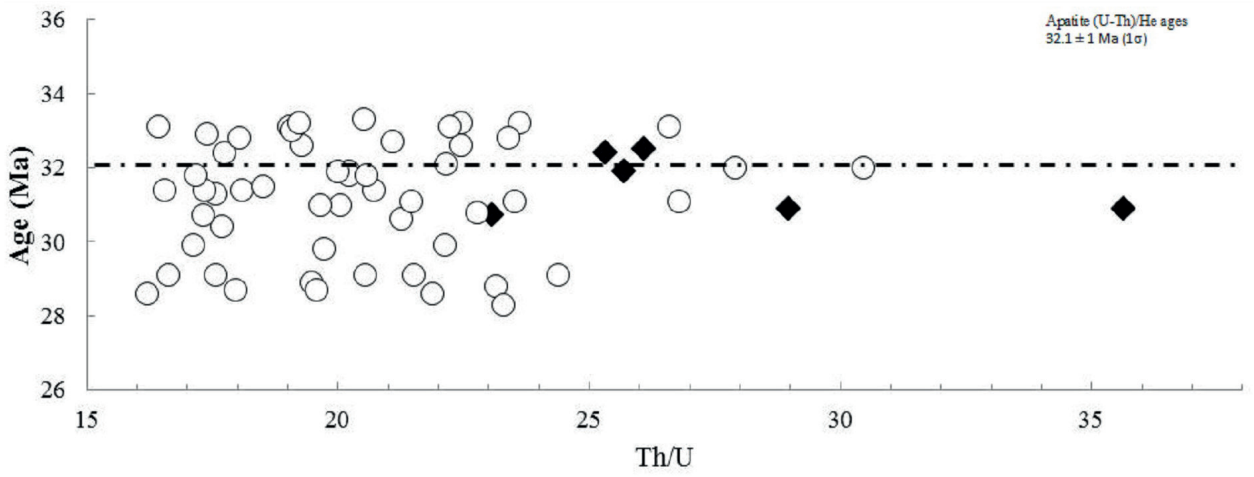


**Figure 5 -** Plot of apatite (U-Th)/He ages versus Th/U. Durango fluorapatite. Black diamonds represent SUERC (EK) Durango; White circles are UNESP Rio Claro DUR UNESP (RC) Durango. Dashed line is Durango fluorapatite He ages of (House et al. 2000) (32.1 ± 1.7 Ma (2σ, n=11).

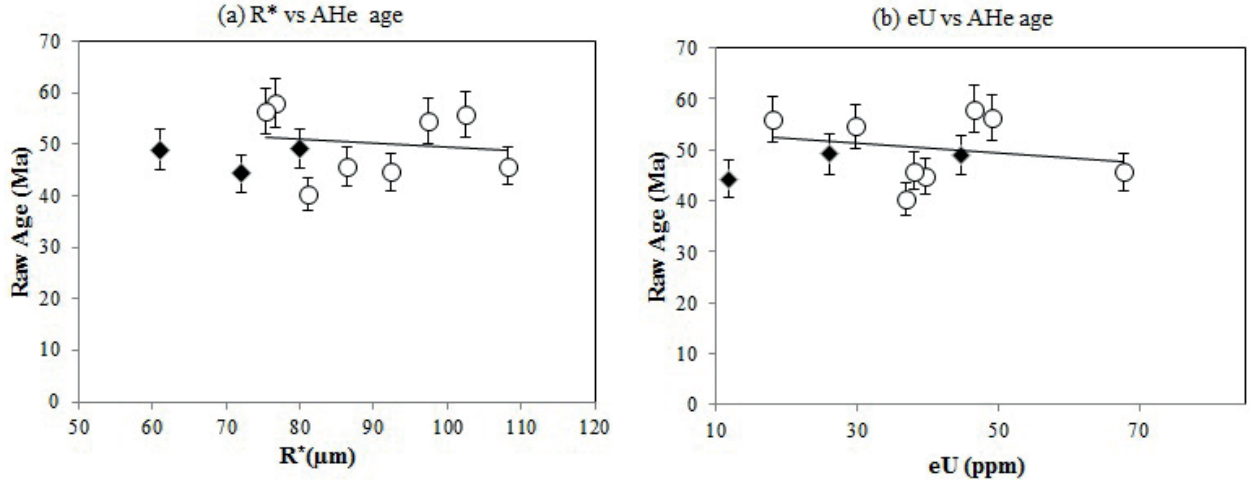


**Figure 6 -** (**a**) Single-grain AHe ages plotted against grain spherical equivalent radius (R*); (**b**) single-grain AHe age plotted against eU (effective uranium; [U ppm] + (0.237*[Th ppm]). White circles and black diamonds circles represent samples analyzed in the Rio Claro and SUERC He laboratories, respectively.

Siqueira-Ribeiro et al. (2011), indicate that the landscape evolution is associated with several distinct exhumation events. Northwest of Rio de Janeiro state, a novel approach to constraining the erosional history of the SM presented by Cogné et al. 2011, 2012, Siqueira-Ribeiro et al. 2011. In these papers, apatite fission track and AHe ages range from 145 to 53 and 75 to 37 Ma, respectively. Forward modelling confirms Late Cretaceous-Paleogene cooling identified earlier by Hackspacher et al. (2004) and Hiruma et al. (2010), recognizing a distinct cooling phase in Neogene, between 30 and 10 Ma. Neogene cooling rapid caused exhumation of rocks 1 km through of the crust mainly in south portion of the SM in the Rio de Janeiro state.

## FUTURE DEVELOPMENTS AND CONCLUSIONS

This study demonstrates that the UNESP He thermochronology laboratory is capable of routine

**TABLE II**

**Results of apatite (U-Th)/He analysis. eU [(a)] (effective uranium) is calculated as [U ppm] + (0.237*[Th ppm]); [(b)] Correction factor after (Farley et al. 1996), assuming homogeneous distribution U and Th; [(c)] Estimate uncertainty is equal to 2σ analytical uncertainty includes U, Th, and He measurement uncertainties; Corrected AHe age = raw AHe age/Ft.**

| | | $^{4}$He | $^{238}$U | | $^{235}$U | | $^{232}$Th | | eU[a] | *R | | Raw Age | ±UC[c] | Corrected Age (Ma) | ±UC[c] | Raw Age | | Corrected Age (Ma) | |
|---|---|---|---|---|---|---|---|---|---|---|---|---|---|---|---|---|---|---|---|
| **Sample** | **Grain** | **(cc)** | **(ng)** | **(ppm)** | **(ng)** | **(ppm)** | **(ng)** | **(ppm)** | **(ppm)** | **(µm)** | **Ft[b]** | **(Ma)** | | **(Ma)** | | **Average** | **SD** | **Average** | **SD** |
| TF-685 (RC) | 2 | 3.88E-09 | 0.354 | 19.64 | 0.003 | 0.17 | 1.51 | 83.95 | 39.53 | 92.3 | 0.84 | 44.7 | 3.4 | 53.4 | 4.06 | 50.2 | 6.7 | 60.5 | 8.7 |
| | 4 | 3.10E-09 | 0.248 | 26.29 | 0.002 | 0.21 | 0.80 | 85.23 | 46.53 | 76.7 | 0.80 | 58.0 | 4.2 | 72.1 | 5.22 | | | | |
| | 5 | 3.99E-09 | 0.301 | 14.91 | 0.002 | 0.1 | 1.26 | 62.56 | 29.71 | 97.4 | 0.85 | 54.6 | 4.1 | 64.5 | 4.85 | | | | |
| | 6 | 3.15E-09 | 0.255 | 27.3 | 0.002 | 0.21 | 0.86 | 92.17 | 49.17 | 75.3 | 0.80 | 56.4 | 4.1 | 70.4 | 5.12 | | | | |
| | 7 | 2.78E-09 | 0.194 | 8.52 | 0.001 | 0.04 | 0.90 | 39.73 | 17.90 | 102.4 | 0.85 | 55.9 | 4.3 | 65.5 | 5.04 | | | | |
| | 8 | 6.27E-09 | 0.567 | 19.2 | 0.004 | 0.14 | 2.36 | 80.02 | 38.14 | 108.2 | 0.86 | 45.8 | 3.5 | 53.2 | 4.07 | | | | |
| | 9 | 2.19E-09 | 0.237 | 19.68 | 0.002 | 0.17 | 0.87 | 72.68 | 36.93 | 81.1 | 0.82 | 40.4 | 3.0 | 49.6 | 3.68 | | | | |
| | 10 | 5.75E-09 | 0.557 | 36.57 | 0.004 | 0.26 | 2.01 | 132.16 | 67.89 | 86.3 | 0.83 | 45.7 | 3.4 | 55.3 | 4.11 | | | | |
| TF-685 (SUERC) | 2 | 5.50E-10 | 0.043 | 4.95 | 0.00 | 0.00 | 0.24 | 28.55 | 11.66 | 72.0 | 0.79 | 44.3 | 1.1 | 56.0 | 1.4 | 47.5 | 2.8 | 59.6 | 3.3 |
| | 3 | 2.10E-09 | 0.157 | 20.08 | 0.00 | 0.00 | 0.81 | 104.5 | 44.64 | 61.0 | 0.79 | 49.0 | 0.9 | 62.3 | 1.1 | | | | |
| | 4 | 1.80E-09 | 0.144 | 12.46 | 0.00 | 0.00 | 0.66 | 57.43 | 25.95 | 80.0 | 0.81 | 49.2 | 0.9 | 60.7 | 1.1 | | | | |

apatite He age measurements to international standard. Routine operation is currently the analysis of one laser pan each week, equivalent to approximately 200 single apatite analyses each month. The laboratory is adjacent to the UNESP Fission Track laboratory, thus the facility provides the full range of low temperature thermochronology techniques for South American research scientists. Future work will involve development of He thermochronology in new minerals (e.g., zircon, Dobson et al. 2008) to allow us a better understanding the regional crustal evolution.

## ACKNOWLEDGMENTS

This study was supported by the Coordenação de Aperfeiçoamento de Pessoal de Nível Superior (CAPES) 081/2012 (Ciências em Fronteiras-Pesquisador Visitante Especial) for financial support to FS. We thank Luigia Di Nicola at Scottish Universities Environmental Research Centre (SUERC); Petrobras Project (Geotectonic network), Conselho Nacional de Desenvolvimento Científico e Tecnológico (CNPq) and FAPESP for financial support to Peter C. Hackspacher, Fundação de Amparo à Pesquisa do Estado de São Paulo (FAPESP) Multiuser Equipment project process: n°2009/54146-0 and Karl Burke in Thermo Fisher for assistance with the Helix-SFT mass spectrometer and training in 2013. We are also grateful to Pieter Veermesch and an anonymous reviewer who provided constructive comments that markedly improved the paper.

## AUTHOR CONTRIBUTIONS

Marli Carina Siqueira-Ribeiro is responsible by development of the apatite (U-Th-Sm)/He method in the paper. Including all aspects of calibration, standard preparation, ion source tune parameters, interpretation of the Uranium effective versus AHe ages and grain ratios. Danieli Fernanda Canaver Marin is responsible by development of the apatite (U-Th-Sm) method in the paper. Including all aspects of calibration, standard preparation, and isotopic ratio and tune parameters. Peter Christian Hackspacher: Geological interpretation on the sample paper's. Finlay M. Stuart: Supervision on all aspects relationed about the development and implantation of the apatite (U-Th-Sm)/He method in the paper.

## REFERENCES

BOYCE JW AND HODGES KV. 2005. U and Th zoning Cerro de Mercado (Durango, Mexico) flourapatite: Insights regarding the impact of recoil redistribution of radiogenic $^{4}$He on (U-Th)/He thermochronology. Chem Geol 219: 216-274.

BROWN RW, BEUCHER R, ROPER S, PERSANO C, STUART F AND FITZGERALD P. 2013. Natural age dispersion arising from the analysis of broken crystals, part I. Theoretical basis and implications for the apatite (U-Th)/He thermochronometer. Geochim Cosmochim Ac 122: 478-497.

COGNÉ N, GALLAGHER K AND COBBOLD PR. 2011. Post-rift reactivation of the onshore margin of southeast Brazil: Evidence from apatite (U-Th)/He and fission-track data. Earth Planet Sc Lett 309: 118-130.

COGNÉ N, GALLAGHER K, COBBOLD PR, RICCOMINI C AND GAUTHERON C. 2012. Post-breakup tectonics in southeast Brazil from thermochronological data and combined inverse-forward thermal history modeling. J Geophys Res 117: 2-16.

DOBSON KG, STUART FM, DEMPSTER J AND EIMF. 2008. U and Th zonation in Fish Canyon Tuff zircon: Implications for a zircon (U-Th)/He standard. Geochim Cosmochim Ac 72: 745-755.

DODSON MH. 1973. Closure temperature in cooling geochronological and petrological systems. Contrib Mineral Petrol 40: 259-274.

EHLERS TA AND FARLEY KA. 2003. Apatite (U-Th)/He thermochronometry: Methods and applications to problems in tectonics and surface process. Earth Planet Sc Lett 206*:* 1-14.

FARLEY K, WOLF R AND SILVER L. 1996. The effects of long alpha stopping distances on (U-Th)/He dates. Geochim Cosmochim Ac 60: 4223-4229.

FARLEY KA. 2002. (U-Th)/He dating: Techniques, calibrations and applications. In: Porcelli DP et al. (Eds), Noble Gases in Geochemistry and Cosmochemistry. Mineralogy Society of America, Washington, DC, USA, p. 819-844.

FARLEY KA, KOHN BP AND PILLANS B. 2002. (U-Th)/He dating of Pleistocene zircon and apatite: A test case from the Rangitawa tephra, North Island, New Zealand. Earth Planet Sc Lett 201: 117-125.

FLOWERS RM, KETCHAM RA, SHUSTER DL AND FARLEY KA. 2009. Apatite (U-Th)/He thermochronometry using a radiation damage accumulation and annealing model. Geochim Cosmochim Ac 73(8): 2347-2365.

FOEKEN JPT, STUART FM, DOBSON K, PERSANO C AND VILBERT D. 2006. A diode laser system for heating minerals for (U-Th)/He chronometry. Geochem Geophy Geosy 7(4): 1-9.

GAUTHERON C, TASSAN-GOT L, BARBARAND J AND PAGEL M. 2009. Effect of alpha-damage annealing on apatite (U-Th)/He thermochronology. Chem Geol 266: 157-170.

HACKSPACHER PC, RIBEIRO LFB, SIQUEIRA-RIBEIRO MC, FETTER AH, HADLER NETO JC, TELLO CES AND DANTAS EL. 2004. Consolidation and break-up of the South American Platform in Southeastern Brazil: Tectonothermal and denudation histories. Gondwana Res 7: 91-101.

HIRUMA ST, RICCOMINI C, MODENESI-GAUTTIERI MC, HACKSPACHER PC, HADLER NETO JC AND FRANCO-MAGALHÃES AOB. 2010. Denudation history of the Bocaina Plateau, Serra do Mar, southeastern Brazil: Relationships to Gondwana breakup and passive margin development. Gondwana Res 18: 674-687.

HOUSE MA, FARLEY KA AND STOCKLI D. 2000. Helium chronometry of apatite and titanite using Nd-YAG laser heating. Earth Planet Sc Lett 183: 365-368.

HOUSE MA, WERNICK EBP AND FARLEY KA. 1998. Dating topography of the Sierra Nevada, California, using apatite (U-Th)/He ages. Nature 396: 66-69.

KIRSTEIN LA, SINCLAIR H, STUART FM AND DOBSON KJ. 2006. Rapid early Miocene exhumation of the Ladakh Batholith, western Himalaya. Geology 34: 1049-1053.

MACAULAY EA, SOBEL EA, MIKOLAICHU KA, KOHN B AND STUART FM. 2014. Cenozoic deformation and exhumation history of the Central Kyrgyz Tien Shan. Tectonics 33: 135-165.

MCDOWELL FW, MCINTOSH W AND FARLEY KA. 2005. A precise $^{40}Ar$ /$^{39}Ar$ reference age for the Durango apatite (U-Th)/He and fission-track dating standard. Chem Geol 2014: 249-263.

MEESTERS AGCA AND DUNAI TJ. 2002. Solving the production-diffusion equation for finite diffusion domains of various shapes: Part I. Implications for low-temperature (U-Th)/He thermochronology. Chem Geol 186(3): 333-344.

MERTEN S, MATENCO L, FOEKEN JP, STUART FM AND ANDRIESSEN PAM. 2010. From nappe-stacking to out-of-sequence post-collisional deformations: Cretaceous to Quaternary exhumation history of the SE Carpathians assessed by low-temperature thermochronology. Tectonics 29: 1-28.

NASDALA L, KENNEDY AK, VALLEY J, VÁCZI T AND REINERS PW. 2013. Sri Lankan Gem Zircon as Reference Material in Analysis and Research. In: Proceedings to 29$^{th}$ Technical Sessions of Geological Society of Sri Lanka, p. 65-68.

PERSANO C, STUART FM, BISHOP P AND BARFOD D. 2002. Apatite (U-Th)/He age constraints on the development of the Great Escarpment, SE Australia. Earth Planet Sc Lett 200: 79-90.

REINERS PW. 2002. (U-Th)/He chronometry experience a renaissance. EOS 83: 21-27.

REINERS PW AND FARLEY KA. 2001. Influence of crystal size on apatite (U-Th)/He thermochronology: an example from the Bighorn Mountains, Wyoming. Earth Planet Sc Lett 188(3): 413-420.

SHUSTER DL, FLOWERS RM AND FARLEY KA. 2006. The influence of natural radiation damage on helium diffusion kinetics in apatite. Earth Planet Sc Lett 249(3): 148-161.

SIQUEIRA-RIBEIRO MC, HACKSPACHER PC, RIBEIRO LFB AND HADLER NETO JC. 2011. Evolução Tectônica e Denudacional da Serra do Mar (SE/Brasil) no limite entre o Cretáceo Superior e Paleoceno, utilizando análises de Traços de Fissão e U-Th/He em apatitas. Rev Bras Geomorf 12(3): 3-14.

WOLF RA, FARLEY KA AND SILVER LT. 1996. Helium diffusion and low temperature thermochronometry of apatite. Geochim Cosmochim Ac 60: 4231-4240.

ZEITLER PK, HERCZIG AL, MCDOUGALL I AND HONDA M. 1987. U-Th-He dating of apatite: a potential thermochronometer. Geochim Cosmochim Ac 51: 2865-2868.